Structural and Functional Changes Occuring During Growth of the Respiratory System Can Be Quantified and Classified

Clara M. Ionescu[1], Dana Copot[1], Hannes Maes[2], Gerd Vandersteen[2], Amélie Chevalier[1] and Robin De Keyser[1]

[1]*Ghent University, Department of Electrical Energy, Systems and Automation, Technologiepark 913, B9052 Zwijnaarde, Belgium*

[2]*Vrije Universiteit Brussel, Department ELEC, Pleinlaan 2, 1050 Brussels, Belgium*

Keywords: Respiratory Impedance, Frequency Response, Nonlinear System, Detection Lines, Spectral Analysis, Forced Ocillation Technique.

Abstract: This paper describes the nonlinear effects in the respiratory signals captured by means of the forced oscillation technique (FOT) non-invasive lung function tests. The measurements are performed using a prototype device developed such that it overcomes the limitations present in commercial FOT devices and allows the generation of multisine signals below 4 Hz. The principle of sending detection lines in the frequency domain for characterizing odd and even nonlinear contributions from a nonlinear system are introduced briefly to the reader. Two detection methods are presented: a robust method based on multiple measurements and a fast method based on a single measurement. The ingenious combination of the device and the method allow to detect the nonlinear contributions in the respiratory signals: pressure and flow. The intrinsicly pesent nonlinear effects are quantified by means of a novel index and analyzed in two groups of healthy volunteers, aged 14 years and aged 17 years, respectively. The results we obtain suggest that the proposed device, method and index are a successful combination of lung function testing, signal processing and classification items.

1 INTRODUCTION

The generic evolution of chronic respiratory disease can be captured in the flowchart from figure 1. Asthma and COPD (chronic obstructive pulmonary disease) originate from the interaction of susceptibility genes and environmental factors that underly the pathogenesis of the diseases. Inflammation, in the broadest sense, is the initiator to the structural and functional changes. These changes have an impact on each other (arrows) and are responsible for the excessive airway narrowing that is the fundamental abnormality leading to symptoms (Northrop, 2010; Ionescu, 2013; De Melo et al., 2000).

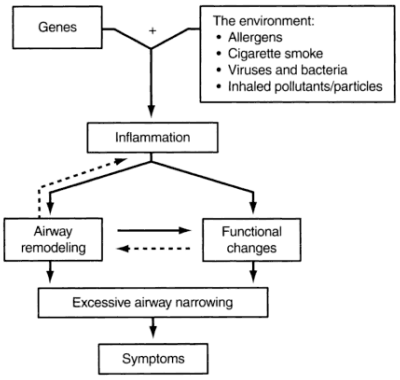

Figure 1: Flowchart of lung inflammation.

Airway remodeling is the process of modification and sustained disruption of structural cells and tissues leading to a new airway-wall structure and functions. The underlying principle of asthma and COPD is caused by concepts in immunology and inflammation. Acute inflammation is the response of vascularized tissue to injury. The reaction is initiated to protect the host and to restore its function and tissue to normal. However, in COPD and asthma occurs a direct switch from episodic, acute to chronic inflammation which results in structural airway remodeling and functional changes. The accelerated decline in lung function is characterized by an alternation in size, mass or number of structural components. Reasons for the persistence of the chronic inflammation are not fully clear. But one generally accepts that dif-

M. Ionescu C., Copot D., Maes H., Vandersteen G., Chevalier A. and De Keyser R..
Structural and Functional Changes Occuring During Growth of the Respiratory System Can Be Quantified and Classified.
DOI: 10.5220/0004729901100115
In *Proceedings of the International Conference on Bio-inspired Systems and Signal Processing* (BIOSIGNALS-2014), pages 110-115
ISBN: 978-989-758-011-6

ferent causes exist. A defect in the repair process, infection, genetically influenced abnormal inflammatory response or repeated inhalation/exposure of allergen/noxious agents are all possible causes (Northrop, 2010; Lutchen, 1988; Suki and Lutchen, 1992).

The exact relationship between airway remodeling and functional changes is not clear yet but functional changes plays also an important role in the progression of chronic lung diseases. This includes the mechanical airway remodeling due to structural changes on macroscopic level and is described in the next chapter. Functional changes will also determine the lung tissue property. Although airway remodeling is supposed to be a consequence of long-term airways diseases, studies (Ionescu, 2013) suggest that the remodeling may be a part of the primary pathology rather than simply a result of chronic inflammation. The remodeling of the airways changes individually and the natural history is not still perfectly understood. known.

In this paper we report the results of a method which enables the quantification of these nonlinear contributions in an objective manner, by introducing a novel index. This index will be evaluated on two groups of healthy children, of two different age groups (i.e. 17 and 19 years old), in order to check that the proposed index is able to capture differences in structure and function between the groups. The paper is organize as follows: the next section presents the method of lung function testing, the method of frequency response evaluation and the novel index. The third section presents the groups of children evaluated in this study and the results obtained. A conclusion section summarizes the outcome of this work and speculates further use of the method.

2 METHODS

2.1 Signal Processing

The fundamental difference between a linear time invariant system and a nonlinear system is that the nonlinear system transfers energy from one frequency in the input signal to other frequencies in the output signal.

The influence of nonlinear distortions on the frequency response function (FRF) measurements are determined by using a random phase multisine (Schoukens and Pintelon, 2001; Schoukens et al., 2005):

$$U(t) = \sum_{k=1}^{N} A_k \cos(k\omega_0 t + \phi_k) \qquad (1)$$

as an input signal, with A_k the non-zero amplitude for odd k values, $\omega_0 = 2\pi f_0$ and $f_0 = 0.1$ Hz, ϕ_k the phase uniformly and independently distributed in the $[0; 2\pi]$ interval and N the number of sinusoids.

The best linear approximation (BLA) of a nonlinear system can be viewed as a minimization of the mean squared error between the true output of the nonlinear system and the output of a linear model. The estimated BLA $\hat{G}_{BLA}(j\omega_k)$ of a wide class of nonlinear systems, obtained using a random phase multisine, can be written as:

$$\hat{G}_{BLA}(j\omega_k) = G_{BLA}(j\omega_k) + G_S(j\omega_k) + N_G(j\omega_k) \quad (2)$$

with $G_{BLA}(j\omega_k)$ the true best linear approximation (BLA) of the nonlinear system, $G_S(j\omega_k)$ the zero mean stochastic nonlinear contributions and $N_G(j\omega_k)$ the measurement noise (Schoukens and Pintelon, 2001). The stochastic nonlinear contributions $G_S(j\omega_k)$ can be extracted by averaging from a manifold of experiments M containing different phase realizations in the excitation signal from (1). The measurement noise $N_G(j\omega_k)$ can be minimized by measuring longer, thus by increasing N.

The basic principles for detecting nonlinearities are shown in figure 2. The output of a linear system, which is excited with a multi-frequency input signal, is given on the first row. Only amplitude variations on the excited (odd) frequencies are observed (red). However, when this input signal is applied on a nonlinear system (e.g. the respiratory tissue), nonlinear dynamics become visible and can be measured as additional detection lines (second and third row in blue and green). These distortions are in fact superimposed to the linear output signal and contribute to the signal measured at the output (last row). The resulting output signal contains extra information via phase differences. The nonlinear contributions can be determined via the identification of the even and odd harmonics (blue and green).

Figure 3 depicts a schematic of the input and output measurements corrupted by noise and the corresponding BLA. In (Schoukens et al., 2005; Zivanovic and Schoukens, 2009), a variance analysis procedure

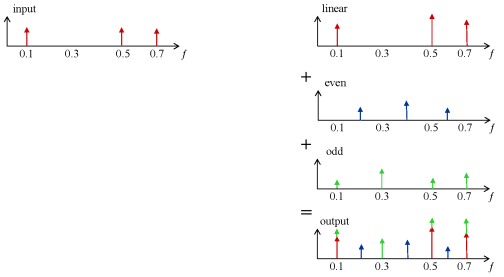

Figure 2: A schematic representation of the input-output contributions.

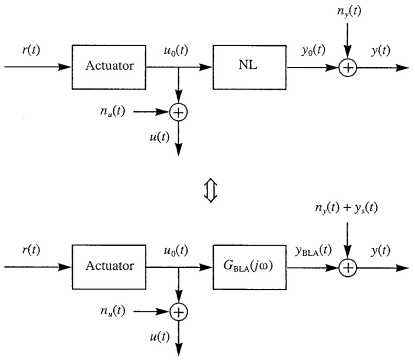

Figure 3: Input $u(t)$ and output $y(t)$ measurements with noise from a nonlinear system driven by an actuator with input signal $r(t)$ (top), and its corresponding best linear approximation (under).

has been proposed that allows to detect and quantify the stochastic nonlinear distortions $G_S(j\omega_k)$ and the disturbing noise $N_G(j\omega_k)$. Two measurement methods can be applied:

- a robust method, which uses different random phase realizations of an odd multisine excitation to get information about the stochastic nonlinear distortions;
- a fast method, which uses only one realization of an odd random phase multisine with random harmonic grid.

The information about the stochastic nonlinear distortions is obtained via the detection lines (non-excited harmonics) in the output DFT spectrum. To compensate for spectral impurity of the input, a first order correction is applied to the output DFT spectrum. The use of an odd random phase multisine with a random harmonic grid provides also a classification of the nonlinear distortions in even and odd contributions in the corrected output DFT spectrum.

Figure 4 shows the principle of measuring the BLA using the robust method, i.e. by averaging between M realizations with P periods. If the input signal is known and uncorrupted with noise, one can obtain the non-parametric estimation of the BLA as $G_{BLA}(j\omega_k)$, the variance of the stochastic nonlinear distortions $var(G_S(j\omega_k))$ and the variance of the noise $\sigma^2_{GBLA,n}$. Given that $n_y(t)$ is a stochastic signal and $y_s(t)$ a periodic signal depending on the phase realization of the input (reference) signal $r(t)$, the frequency response function of the m^{th} realization and p period, $G^{[m,p]}(j\omega_k)$ can be written as:

$$G^{[m,p]}(j\omega_k) = G_{BLA}(j\omega_k) + \frac{Y_S^{[m]}(k)}{U_0^{[m]}(k)} + \frac{N_Y^{[m,p]}(k)}{U_0^{[m]}(k)} \quad (3)$$

Next, the BLA, variance of the nonlinear distortions

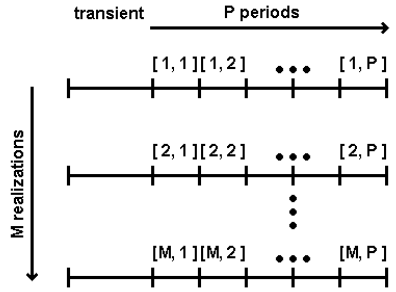

Figure 4: Measurement procedure for the robust method: P periods of length N measured from the steady state response with an odd multisine input. The experiment is then repeated M times, each time with a different odd random phase multisine realization.

and noise variance can be estimated as:

$$\hat{G}^{[m]}(j\omega_k) = \frac{1}{P}\sum_{p=1}^{P} G^{[m,p]}(j\omega_k) \quad (4)$$

$$\hat{G}_{BLA}(j\omega_k) = \frac{1}{M}\sum_{m=1}^{M} \hat{G}^{[m]}(j\omega_k) \quad (5)$$

$$\hat{\sigma}^2_{\hat{G}^{[m]}}(k) = \sum_{p=1}^{P} \frac{|G^{[m,p]}(j\omega_k) - \hat{G}^{[m]}(j\omega_k)|^2}{P(P-1)} \quad (6)$$

$$\hat{\sigma}^2_{\hat{G}_{BLA}}(k) = \sum_{m=1}^{M} \frac{|G^{[m]}(j\omega_k) - \hat{G}_{BLA}(j\omega_k)|^2}{M(M-1)} \quad (7)$$

$$\hat{\sigma}^2_{\hat{G}_{BLA,n}}(k) = \frac{1}{M^2}\sum_{m=1}^{M} \hat{\sigma}^2_{\hat{G}^{[m]}}(k) \quad (8)$$

$$var(G_S(j\omega_k)) \approx M(\hat{\sigma}^2_{\hat{G}_{BLA}}(k) - \hat{\sigma}^2_{\hat{G}_{BLA,n}}(k)) \quad (9)$$

Nomenclature:

- $U_0^{[m]}(k)$ - input of DFT spectra of m^{th} FRF measurements;
- $Y^{[m,p]}(k)$ - output of DFT spectra of m^{th} FRF measurements;
- $G_{BLA}(j\omega_k)$ - asymptotic best linear approximation;
- $\hat{G}^{[m]}(j\omega_k)$ - estimated spectrum of m^{th} realizations;
- $G^{[m,p]}(j\omega_k)$ - frequency response function;
- P - number of periods;
- $\hat{G}^2_{BLA}(k)$ - estimation of best linear approximation;
- $\hat{\sigma}^2_{\hat{G}_{BLA}}(k)$ - estimation of the total variance averaged over M experiments;
- $\hat{\sigma}^2_{\hat{G}_{BLA,n}}(k)$ - the variance of noise averaged over M experiments;

- $var(G_S(j\omega_k))$ - variance of the stochastic nonlinear distortions with respect to one multisine realization.

The total variance and noise variance averaged over the M experiments give an indication upon the reliability of the measured frequency response functions. The variance of the stochastic nonlinear distortion for each realization gives an indication of how much distortion is present in the system with each experiment.

The fast method can be considered as a special case of the robust method, with $M = 1$. As such, the variance is expected to have higher values and less reliability for the fast method than in the robust method. For all the results presented in this paper, the robust method was employed with $M = 5$. Fast method needs odd detection lines and approximation in order to predict the odd distortion levels at the exited bins.

2.2 Signal Measurement

The standard (commercialized) forced oscillation technique (FOT) is a non-invasive technique which applies small air pressure oscillations to the respiratory system of a subject who is breathing spontaneously (Oostveen et al., 2003; Smith et al., 2005). The pressure oscillations are generated by means of a loudspeaker or a fan connected to a chamber. The loudspeaker, or the fan, is driven by a power amplifier fed with the oscillating signal $u(t)$ generated by a computer, which generates a pressure oscillation inside the chamber. This air pressure oscillation is applied to the respiratory system by means of a tube connecting the chamber and an anti-bacterial filter. There is always fresh air in the system through the design of the device. Pressure $p(t)$ and flow $q(t)$ are measured at the mouthpiece with the combination of two pressure sensors and a pneumotachograph. The excitation pressure signal is kept within a range of a peak-to-peak size of $0.1 - 0.3\ kPa$, typically for patient safety, comfort and to ensure linearity.

Based on earlier developments (Ionescu et al.,), an improved, novel (prototype) device was designed for a lower frequency range than the standard FOT device (Maes et al., 2013). Lower frequencies hold valuable information from medical point of view, since they are closer to the breathing signal and thus give valuable information about the respiratory mechanics in the frequency range of the breathing ($0.1 - 0.3\ Hz$). The details of the prototype device and the design of the excitation signal have been given in (Maes et al., 2013).

2.3 Novel Index for Nonlinear Contributions

In order to quantify these nonlinear contributions, the following index has been introduced in (Ionescu, 2013):

$$T = \frac{P_{even} + P_{odd}}{P_{exc}} \cdot \frac{U_{exc}}{U_{even} + U_{odd}} \tag{10}$$

where P represent the pressure and U is the input signal.

Each variable is the sum of the absolute values of all the contributions in pressure signal and input flow signal respectively, at the even non-excited frequencies, the odd non-excited frequencies and the excited odd frequencies. Only the corrected output pressure has been taken into account when calculating (10), i.e. the linear contribution has been estimated and subtracted.

This index expresses a relative ratio of the contributions at the non-excited frequency points, with respect to the contributions at the excited frequency points. Furthermore, it gives a relative measure of the gain between contributions in the input and in the output of the system. Since this is a nonlinear system whose output depends on the input, the choice for this relative measure is technically sound.

2.4 Healthy Volunteers

The measurement campaign was performed at Ghent University, Campus Ardoyen, during the event of the 'Science Week' organized in our department. The children have been performing measurements after apriori signing a written informed consent, further supported by a responsible adult (i.e. the teacher who was responsible for their visit). Also each patient has fill in a form regarding their health status. The biometric data for the healthy groups are given in table 1, with values given as mean with standard deviations. Their respiratory values have been successfully validated as healthy, with reference values for respiratory impedance measured by FOT using the prediction models from (Northrop, 2010; Ionescu, 2013). Hence, the information gathered in this report will discuss differences based solely on structural changes between the two age groups as a result of growth.

3 RESULTS AND DISCUSSION

The results of the two groups evaluated by means of the index from (10) are given in figure 5 as boxplots. The choice for boxplots is motivated by the fact that

Table 1: Biometric parameters of the investigated healthy subjects.

	14-years (20)	17-years (158)
Male/Female	1/19	96/61
Age (yrs)	14±0.3	17±0.6
Height (m)	1.63 ± 0.05	1.74 ± 0.08
Weight (kg)	48±8	62±9
BMI	18±2	20±2

it is a straightforward statistical measure providing outlier percentage score and mean value within each group. Statistically meaningful differences between groups are present if the p value is lower than 0.05 (i.e. 95% confidence intervals). For the data measured and examined in this study, we obtained a p value of 0.0158, which indicates that the proposed index is able to capture differences originated by the variations in the structure of the respiratory system with growth.

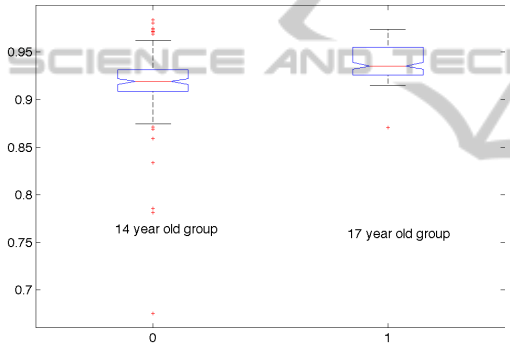

Figure 5: Boxplot of the nonlinear contributions in the two groups.

Changes in structure and in the respiratory airways and tissue with growth lead to changes in overall dynamics and mechanical properties. The dynamics change because of the novel path that air has to pass during inspiration-expiration process of breathing. Since there are structural changes, the air will have various aerodynamic properties. The changes in the material properties of the airway and tissue will also have an effect on these aerodynamic properties, e.g. resistance or elasticity of the airways will produce various response to air pressure oscillations. By measuring with FOT the air pressure and air flow involved during unforced breathing, one is able to characterize the transfer function (i.e. impedance) of the dynamic respiration (Daroczi and Hantos, 1982; Ionescu and De Keyser, 2003). By using the special detection line algorithm presented in section 2.1, it is possible to separated nicely the linear from the nonlinear contributions in this dynamic process. The result from figure 5 supports this theory and shows distinctly the added value of the novel index. It should be noted that to date, there is no other clinical measure of nonlinear distortion amount in the respiratory system.

One may speculate that the nonlinear distortions tend to be significantly increased in patients diagnosed with respiratory disease than in healthy subjects. From clinical insight, this is indeed a valid conclusion (recall here structural changes discussed in the introduction of the paper). For instance, the respiratory system affected by cystic fibrosis is filled with viscous secretions which will change the heterogeneous appearance of the tissues and introduce nonlinear effects originated by turbulent flow, viscoelasticity, excessive inflammation and clogged airways. The respiratory system affected by asthma is subject to airway hyper-responsiveness leading to airway chronic inflammation. This affects the airway remodeling, changing airflow dynamics and hence introducing nonlinear effects from turbulent flow, airway obstruction, airway muscle fibrosis etc. In both cases, changes in structure and morphology will change the nonlinear behavior of the respiratory system, hence the values of the proposed index are expected to change as well.

This preliminary evaluation was performed on a reasonably large number of healthy volunteers, and it suggests that measuring nonlinear contributions may be beneficial to gather insight into the evolution of respiratory diseases. The fact that respiratory mechanics at low frequencies have inherent information on the viscoelastic properties of airways and tissue is motivating the development of signal processing algorithms which can cancel the interference with the breathing of the patient. The challenge is that the amplitude and frequency of the breathing signal may vary within the measurement and from one measurement to another, making the detection lines prone to biased values. The results obtained in these initial steps are a proof of concept which motivates further development of the FOT device and the detection algorithm.

4 CONCLUSIONS

This paper presented an integrated approach for detection of nonlinear distortions present in the breathing dynamics as a result of structural and material properties. As a preliminary study, the information gathered here is crucial for the further development and implementation of measuring devices and algorithms to measure low-frequency respiratory impedance in a non-invasive and simple man-

ner, without requiring breathing maneuvers or complex respiratory tests. The results obtained in these initial steps are a proof of concept for the added value of FOT within the clinical onset and motivates further development of the detection algorithm. Future work will include large scale measurements in patient groups with a wide range of age and a gender balance. This experiments will help quantify whether a patient has asthma or COPD based on respiratory measurements using the less-invasive FOT device.

ACKNOWLEDGEMENTS

The authors are grateful for to Mr Stig DOOMS for performing the measurements, and to Miss Amelie CHEVALIER for organizing the measurement campaign. This work is sponsored by Ghent University, Vrije Universiteit Brussel and the Foundation for Scientific Research (FWO- Vlaanderen), Belgium.

REFERENCES

Daroczi, B. and Hantos, Z. (1982). An improved forced oscillatory estimation of respiratory impedance. *International Journal of Bio-Medical Computing*, 13:221–235.

De Melo, P., Werneck, M., and Giannella-Neto, A. (2000). Effect of generator nonlinearities on respiratoy impedance. *Medical and Biological Engineering and Computing*, 38:102–108.

Ionescu, C. (2013). *The human respiratory system: an analysis of the interplay between anatomy, structure, breathing and fractal dynamics*. Springer, Series in Bio-Engineering.

Ionescu, C. and De Keyser, R. (2003). A novel parametric model for the human respiratory system. *Proceedings of the IASTED International Conference on Modeling and Simulation.*, pages 246–251.

Ionescu, C., Vandersteen, G., Schoukens, J., Desager, K., and De Keyser, R. Measuring nonlinear effects in respiratory mechanics: a proof of concept for prototype device and method. *IEEE Transaction on Measurement and Instrumentation*.

Lutchen, K. (1988). Optimal selection of frequencies for estimating parameters from respiratory impedance data. *IEEE Transaction on Biomedical Engineering*, 35(8).

Maes, H., Vandersteen, G., Muehlebach, M., and Ionescu, C. (2013). A ventilator-based, low-frequent, forced oscillation technique apparatus. *IEEE Transactions on Measurement and Instrumentation*.

Northrop, R. (2010). *Non-invasive measurements and devices for diagnosis*. CRC Press.

Oostveen, E., MacLeod, D., Lorino, H., Farre, R., Hantos, Z., Desager, K., and Marchal, F. (2003). The forced forced oscillation technique in clinical practice: methodology, recommendations and further developments. *European Respiratory journal*, 22:1026–1041.

Schoukens, J. and Pintelon, R. (2001). *System identification. A frequency domain approach*. IEEE Press.

Schoukens, J., Pintelon, R., Dobrowiecki, T., and Rolain, Y. (2005). Identification of linear systems with nonlinear distorsions. *Automatica*, 41:491–504.

Smith, H., Reinhold, P., and Goldman, M. (2005). Forced oscillation technique and impulse oscillometry. *European Respiratory Monograph*, 31(72):105.

Suki, B. and Lutchen, K. (1992). Pseudorandom signals to estimate apparent transfer and coherence functions of nonlinear systems - applications to respiratory mechanics. *IEEE Transactions Biomedical Engineering*, 39(11).

Zivanovic, M. and Schoukens, J. (2009). Time-variant harmonic signal modeling by using polynomial approximation and fully automated spectral analysis. *Proceedings of the 17th European Signal Processing Conference*.